doi:10.1006/jmbi.2000.3605 available online at http://www.idealibrary.com on IDEAL® *J. Mol. Biol.* (2000) **297**, 733–745

JMB

Measurements of Cysteine Reactivity during Protein Unfolding Suggest the Presence of Competing Pathways

S. Ramachandran, Bhadresh R. Rami and Jayant B. Udgaonkar*

National Centre for Biological Sciences, Tata Institute of Fundamental Research, UAS-GKVK Campus, Bangalore 560065, India

**Corresponding author*

Evidence that proteins may unfold utilizing complex competing pathways comes from a new pulse-labeling protocol in which the change in reactivity of a single cysteine residue in a protein during unfolding is measured, making use of its easily monitored reaction with the Ellman reagent, dithionitrobenzoic acid. The kinetics of unfolding of two single cysteine-containing mutant forms of the small protein barstar, C82A, which contains only Cys40, and C40A, which contains only Cys82, have been studied. The data suggest that unfolding occurs *via* two parallel pathways, each forming competing intermediates. In one of these early intermediates, Cys40 and Cys82 are already as reactive as they are in the fully unfolded protein, while in the other intermediate, the Cys thiol groups are unreactive. One more long-lived intermediate also needs to be included on the pathway defined by the early intermediate with unreactive Cys thiol groups to account for the difference in the rates of fluorescence change and of change in Cys40 reactivity. The demonstration of multiple intermediates and pathways for unfolding indicates that protein unfolding reactions can be as complex as protein folding reactions.

Keywords: pulse-labeling; protein unfolding; competing pathways; barstar; cysteine reactivity

Introduction

Statistical models of protein folding suggest that a large energy landscape is initially accessible to unfolded protein molecules for folding (Bryngelson & Wolynes, 1987; Bryngelson *et al*., 1995; Dill & Chan, 1997; Chan & Dill, 1998; Pande *et al*., 1998; Sali *et al*., 1994). From the energy landscape perspective, it is therefore not surprising that folding reactions may be two-state, or multi-state with the accumulation of folding intermediates, and may utilize multiple competing pathways. A similarly complex energy landscape is likely to be available to folded protein molecules for unfolding (Dill & Chan, 1997; Chan & Dill, 1998; Pande *et al*., 1998), and the unfolding reaction would then be expected to be characterized by the same degree of complexity as is the folding reaction. Thus, from the energy landscape perspective, protein molecules may traverse the energy surface in many different ways during unfolding, and the unfolding reaction may also occur through multiple pathways that could be either two-state, or multi-state with the accumulation of unfolding intermediates. Nevertheless, it is still commonly believed that although proteins might refold *via* specific intermediates, unfolding occurs without the accumulation of intermediates.

The question of whether proteins unfold *via* intermediates has been actively addressed only in the past few years. Kinetic intermediates have been shown to exist on the unfolding pathway of ribonuclease A (Kiefhaber *et al*., 1995; Phillips *et al*., 1995), *Escherichia coli* dihydrofolate reductase (Hoeltzli & Frieden, 1995), and barstar (Nath *et al*., 1996; Zaidi *et al*., 1997; Bhuyan & Udgaonkar, 1998). The occurrence of unfolding intermediates has also been suggested by equilibrium hydrogen exchange measurements in the case of several proteins, including oxidized and reduced cytochrome *c* (Bai *et al*., 1995; Xu *et al*., 1998; Bhuyan & Udgaonkar, 2000) and barstar (Bhuyan & Udgaonkar, 1999a). Structural information about unfolding intermediates will result in characterization of the transition state for unfolding, which is thought to lie close to the native state (Goldenberg & Creighton, 1985; Segawa & Sugihara, 1984a,b).

Abbreviations used: DTNB, dithionitrobenzoic acid.

E-mail address of the corresponding author: jayant@ncbs.res.in

0022-2836/00/030733–13 $35.00/0

Various spectroscopic techniques have been used to monitor the formation or loss of structure during folding or unfolding, respectively. Of the various techniques used to date, the only technique which gives direct information about the status of individual residues in the milliseconds to seconds to s time domain is pulse-labeling by hydrogen exchange (Udgaonkar & Baldwin, 1988; Roder *et al*., 1988). The hydrogen exchange method, although very useful in characterizing intermediates, suffers from several drawbacks: (i) it is biased towards identification of native-like structure. For instance, although hydrogen exchange methods provide direct information on only one of the partners of a hydrogen bond, it is always assumed that the other partner in a folding intermediate is always the same as that in the fully folded protein; (ii) it does not provide information on the surface topology because surface amide hydrogen atoms are invariably inaccessible for study; and (iii) the exchange reaction itself cannot be monitored directly.

Cysteine residues in proteins serve as excellent probes for studying both the structure and kinetics of folding of proteins. This is because the thiol group containing side-chains of cysteine residues are the most reactive of all the amino acid side-chains. One of the earliest studies on the use of the reactivity of cysteine residues for studying protein folding was the equilibrium unfolding and refolding of the constant fragment of the immunoglobulin light chain (Goto & Hamaguchi, 1982). Subsequently, there have been reports on pulse-labeling of cysteine residues to probe for refolding intermediates in yeast phosphoglycerate kinase (Ballery *et al*., 1993) and apomyoglobin (Ha & Loh, 1998).

Barstar, a protein comprised of 89 amino acid residues, has been used extensively as a model system for studying protein folding and unfolding (Bhuyan & Udgaonkar, 1999a; Schreiber & Fersht, 1993; Shastry *et al*., 1994; Shastry & Udgaonkar, 1995; Agashe & Udgaonkar, 1995). Stopped-flow circular dichroism (CD) and fluorescence studies on wild-type and mutant proteins have shown that the unfolding of barstar occurs *via* at least two competing pathways (Nath *et al*., 1996; Zaidi *et al*., 1997):

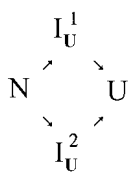

Scheme 1.

The intermediates, I_U^1 and I_U^2 form rapidly on two parallel pathways. It was suggested that on each pathway, a rapid pre-equilibrium is established between N and I_U^1 and/or I_U^2 before either intermediate can unfold to U. In this mechanism, the $N \rightleftharpoons I_U^1$ equilibrium, as well as the $N \rightleftharpoons I_U^2$ equilibrium, is dependent on temperature and GdnHCl concentration. The results suggested that I_U^1 is largely devoid of secondary structure but has an intact core, while I_U^2 is characterized by a solvent-exposed hydrophobic core but still possesses secondary structure.

Wild-type barstar has cysteine residues at positions 40 and 82 along the sequence of the protein, which do not form a disulfide bond (Ramachandran & Udgaonkar, 1996). In this study, two single cysteine-containing mutant forms of barstar have been studied: C82A, in which only Cys40 is present, and C40A, in which only Cys82 is present. A crystal structure of the C82A protein is available (Ratnaparkhi *et al*., 1998) and the structure is quite similar to the solution structure of wild-type barstar (Lubienski *et al*., 1994). Cys40 is 95 % buried in the native state of the protein, while Cys82 is 75 % buried (Figure 1).

Here, we report the use of a novel pulse-labeling strategy for probing the structure of unfolding intermediates at the level of individual amino acid residues. This technique monitors the reactivity of a buried Cys residue (Cys40 in C82A, and Cys82 in C40A) during unfolding, making use of its easily monitored reaction with the Ellman reagent, dithionitrobenzoic acid (DTNB). Reactivity is measured by determining the extent, as well as rate of labeling, of the cysteine thiol group upon reaction with DTNB. It is shown that the change in reactivity of Cys40 in C82A, as well as of Cys82 in C40A, occurs in two kinetic phases: an unobservable rapid burst phase, in which either Cys thiol group becomes as reactive as it is in fully unfolded protein in about 30-50 % of the molecules, and a slower observable phase, in which the remaining molecules unfold. For C82A, the rate of the observable phase is faster when monitored by tryptophan fluorescence than by change in reactivity of the Cys40 thiol group, while for C40A, the rate of the observable phase is the same whether monitored by tryptophan fluorescence or by the change in reactivity of the Cys82 thiol group. These results strongly suggest the presence of two competing pathways of unfolding.

Results

Fluorescence monitored kinetics of unfolding

The kinetics of unfolding of C82A as well of C40A monitored by intrinsic tryptophan fluorescence are different at pH 8.5 and 7.0, although the stabilities of either protein at the two pH values are similar. For C82A, C_m at pH 7.0 is 4.0 M and at pH 8.5 is 3.6 M, while for C40A, C_m at pH 7.0 is 4.3 M and at pH 8.5 is 4.05 M. Figure 2(a) and (b) show the superposition of the kinetic start and end-points on the equilibrium curve for unfolding of C82A at pH 8.5 and 7.0, respectively, while Figure 2(c) and (d) show the superposition of the

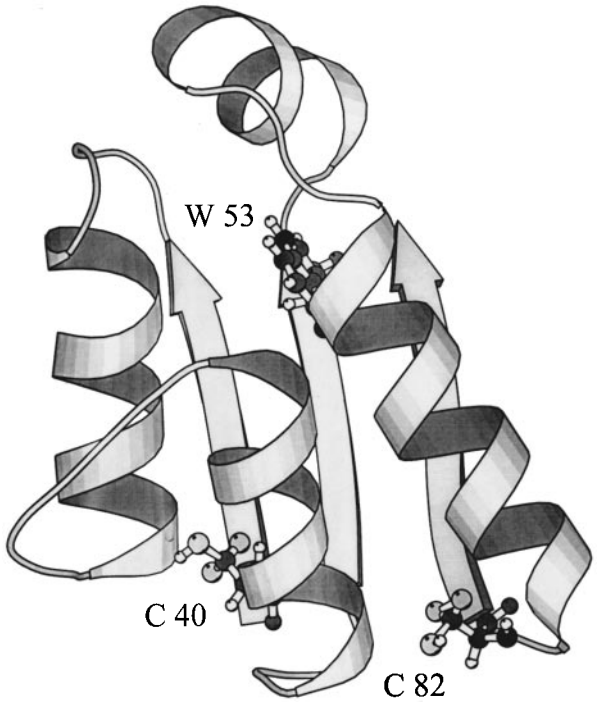

Figure 1. Solution structure of wild-type barstar. Cys40 and Cys82 are 95% and 75% buried. The Figure was drawn using MOLSCRIPT (Kraulis, 1991).

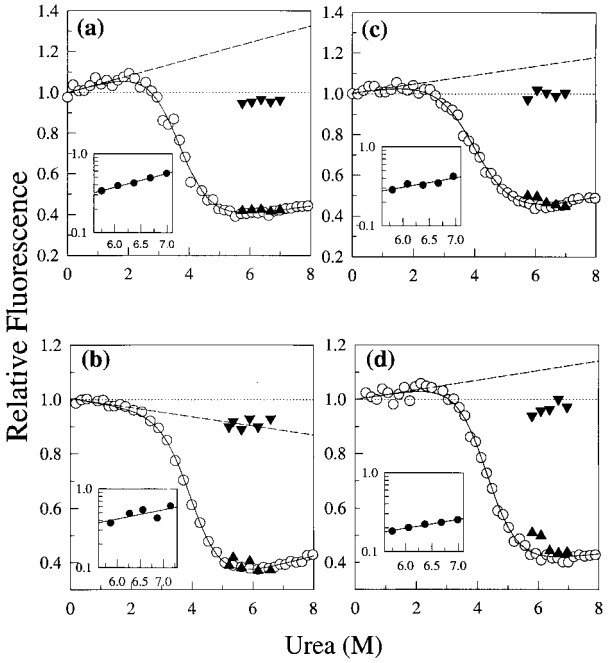

Figure 2. Kinetics of unfolding of C82A and C40A at 25 °C. Kinetic *versus* equilibrium amplitudes of the urea-induced unfolding of (a) and (b) C82A, and (c) and (d) C40A at (a) and (c) pH 8.5, and (b) and (d) pH 7.0. Unfolding was monitored by intrinsic tryptophan fluorescence. (○) equilibrium unfolding curve; (▼) starting point of the kinetic unfolding curve, obtained by extrapolation to $t = 0$; (▲) end-point of the kinetic unfolding curve, obtained by extrapolation to $t = \infty$. All amplitudes are relative to a value of 1 for the native protein. The mid-points of the equilibrium unfolding curves are at 3.6 M and 4.0 M urea at pH 8.5 and 7.0, respectively, for C82A; and at 4.05 M and 4.3 M urea at pH 8.5 and 7, respectively for C40A. In each panel, the broken line is the estimated value of the optical signal of N obtained by linear extrapolation from the folded protein baseline; and, the dotted line represents the optical signal of N, assuming no dependence on denaturant concentration. Insets show the dependence on urea concentration of the observed rate constants for the unfolding of C82A and C40A, monitored by intrinsic tryptophan fluorescence at pH 8.5 as well as pH 7.0.

kinetic start and end-points on the equilibrium curve for unfolding of C40A at pH 8.5 and 7.0, respectively. In all cases, the end-points of the kinetic experiments reproduce the equilibrium signals. For C82A, it appears that there is a 10 ms (which corresponds to the dead-time of stopped-flow mixing) burst phase change in fluorescence, shown by the start-points of the kinetic experiments not falling on the linearly extrapolated native baseline, in the kinetic experiment at pH 8.5, but not at pH 7.0. This would suggest the accumulation of at least one unfolding intermediate at pH 8.5, but not at pH 7.0. For C40A, there appears to be burst phase changes in fluorescence at both pH 7.0 and pH 8.5, suggesting that an unfolding intermediate accumulates at both pH values.

For both proteins, the rates of unfolding at pH 8.5 are marginally faster than the rates at pH 7.0 (Figure 2(a)-(d), insets). All unfolding experiments have been carried out using concentrations of urea that completely unfold the protein. The unfolding reaction of barstar shows two kinetic phases in the folding transition zone, with the slower phase corresponding to the isomerization of the Tyr47-Pro48 peptide bond, which is in the *cis* conformation in the native state (Schreiber & Fersht, 1993; Shastry *et al.*, 1994). The amplitude of this slow phase, which has rates of approximately 0.01 s^{-1}, decreases with increasing denaturant concentrations, and has zero amplitude at high denaturant concentrations in the post transition zone. Therefore, the kinetic phase that is observed here, as well as the fast unobservable burst phase represent structural events during unfolding.

Cysteine reactivities in native and unfolded proteins

Figure 3(a) shows the reaction of Cys40 in C82A under native conditions, and Figure 3(b) shows the reaction of Cys40 under conditions where the protein is fully unfolded. It is observed that Cys40 in C82A reacts 1000-fold more slowly under native conditions (second order rate constant of 2.2 M^{-1} s^{-1}) than under unfolding conditions (second order rate constant of 2300 M^{-1} s^{-1} in 5.8 M urea). Similarly, Cys82 in C40A reacts 1000-fold more slowly

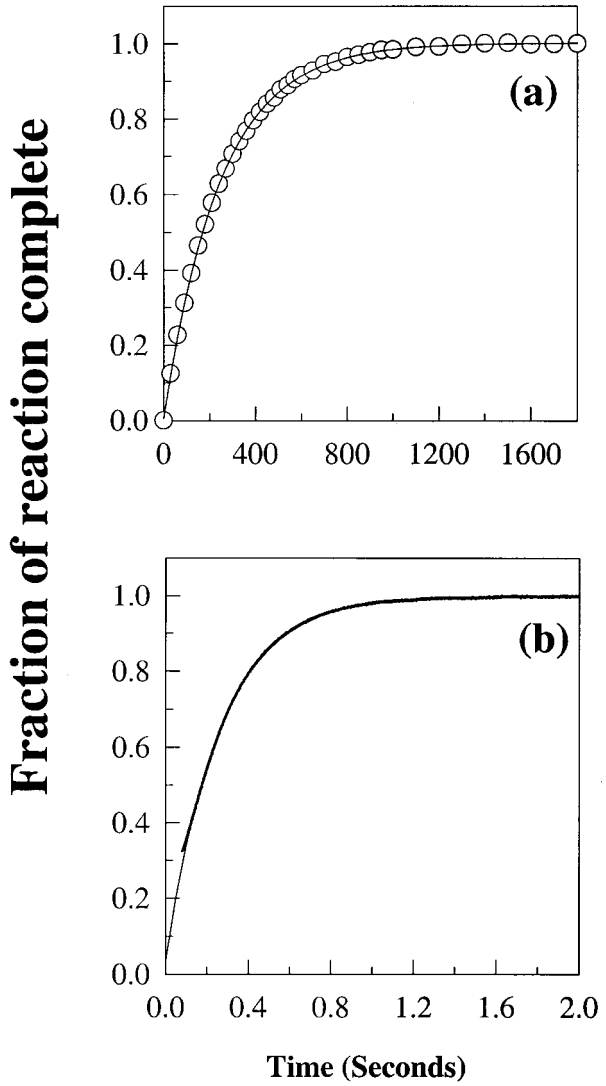

Figure 3. Reaction of DTNB with Cys40 in C82A. (a) Reaction with protein in native buffer at pH 8.5. (b) Reaction in 6.1 M urea. The lines through the data are single exponential fits to the data, which yield observed rates of 0.004 s^{-1} and 3.8 s^{-1} for the folded and unfolded proteins, respectively.

under native conditions (second order rate constant of 1.8 M^{-1} s^{-1}) than under unfolding conditions (second order rate constant of 2900 M^{-1} s^{-1} in 5.8 M urea) (data not shown). For both proteins, the rate measured in unfolding conditions decreases very marginally with increasing urea concentrations (data not shown). Thus, there is a wide difference in the reactivity of either Cys thiol group under native conditions, where it is buried, and unfolding conditions, where it is assumed to be fully exposed to solvent.

Cysteine-labeling reactions

Figure 4(a) shows the extent of the labeling reaction with time, in a direct unfolding experiment, when C40A is diluted directly into a solution containing 6.7 M urea (final) and 1.5 mM DTNB (final concentration). The reaction of DTNB with Cys82 is found to be biphasic, with 50 % of cysteine thiol groups in the protein molecules reacting with a rate of 3.6 s^{-1}, which corresponds to the rate of reaction of 1.5 mM DTNB with C40A unfolded to equilibrium in 6.7 M urea. The other 50 % of molecules react at a rate of 0.2 s^{-1}, which corresponds to the rate of unfolding of C40A in 6.7 M urea (Figure 2). This result suggests that half of the protein molecules have unfolded and therefore become reactive with DTNB in the dead-time (6 ms) of stopped-flow mixing, while the remaining molecules become reactive only as they unfold over the 30 second time domain.

Figure 4(b) shows the reaction of Cys82 in C40A with DTNB, when the labeling reaction is initiated at different times of unfolding in 6.1 M urea. As expected, the observed amplitude of the reaction of DTNB with the Cys thiol group increases with increasing unfolding times. At any time of unfolding, the entire amplitude (±10 %) of the reaction of the Cys thiol group with DTNB is captured. For C40A, as well as for C82A (data not shown), the rate of the reaction of the Cys thiol group with DTNB at any time of unfolding is the same as the rate of the reaction of DTNB with the Cys thiol group in fully unfolded protein. Figure 4(b) makes another important point: the rate of the labeling reaction is fast compared to the rate of the unfolding reaction.

Figure 5 shows typical time-courses of the pulse-labeling experiments with C82A (Figure 5(a)) and C40A (Figure 5(b)) for unfolding in 6.7 M urea. Observable data fit best to a single exponential in each case. When extrapolated to $t = 0$, the fits suggest that 30-60 % of the protein molecules become fully accessible to labeling of the Cys thiol group in a burst phase, and that the remaining 40-70 % of the protein molecules become fully accessible for labeling at the Cys thiol group in the observable kinetic phase. The molecules that become reactive in the burst phase do in fact get labeled initially, when unfolding is initiated in the presence of DTNB (Figure 4(a)).

The data in Figures 4 and 5 suggest that an unfolding intermediate accumulates in the burst phase, in which the Cys thiol group has become reactive. Since all protein molecules do not become reactive in the burst phase, to what is essentially an irreversible chemical modification, the rate of reversion of this intermediate to the native form must be slow compared to the rate of subsequent unfolding reactions. More importantly, a competing pathway along which native molecules can unfold at comparably fast rates must also be available for native protein molecules to traverse. The diversion of a significant fraction of the unfolding molecules to the competing pathway, in which there is no thiol-reactive burst phase intermediate, would account for the observation that only some

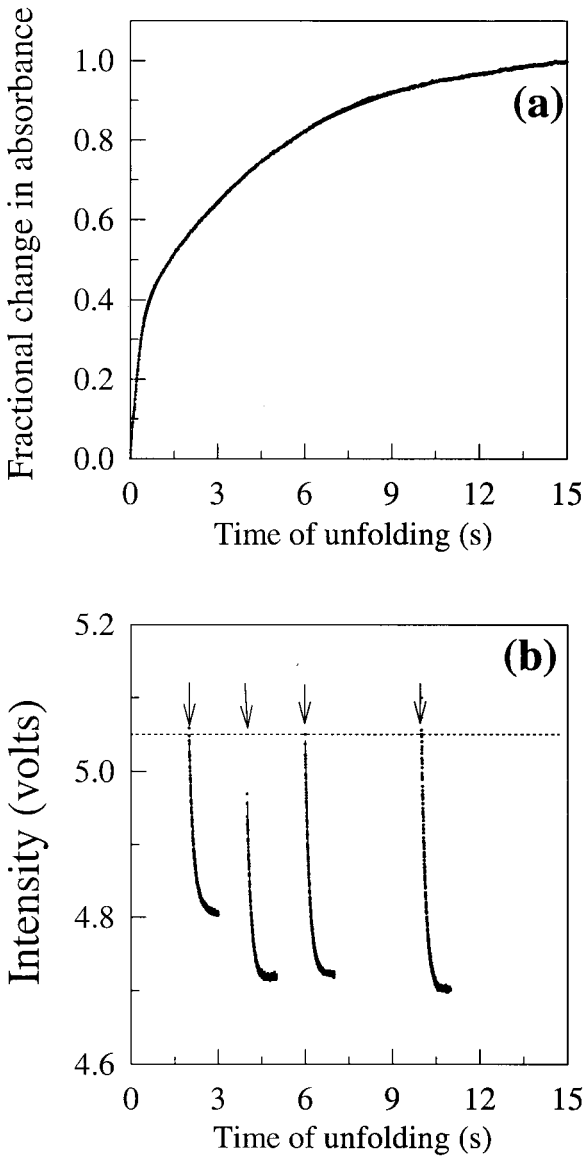

Figure 4. Unfolding of C40A studied by measurement of the reactivity of Cys82. (a) C40A was diluted directly into a buffer containing 6.7 M urea and 1.5 mM DTNB. The change in exposure of Cys82 during unfolding, as measured by the change in absorbance at 412 nm, occurs in two kinetic phases. It is best described by the following expression: $F(t) = Y(0) + A_1 \exp(-k_1 t) + A_2 \exp(-k_2 t)$, where $F(t)$ is the fractional increase in absorbance at 412 nm at time t. (b) Unfolding of C40A was monitored by pulse labeling of Cys82 at different times after commencement of unfolding. C40A was unfolded in 6.1 M urea. Raw data, namely the intensity of transmitted light at 412 nm *versus* time of unfolding (or duration of pulse) are shown. Arrows denote the time of adding DTNB to the unfolding protein solution. In each case, data from four experiments in which a pulse of DTNB was given at two, four, six and ten seconds after commencement of unfolding are shown together. Each exponential trace represents the reaction of the Cys thiol group with DTNB, after different times of unfolding. The broken line shows the baseline with only DTNB. It is seen that all traces begin essentially from the baseline, the rates of labeling (obtained by fitting the resultant changes in absorbance to single exponentials) are independent of time of application of the labeling DTNB pulse and were the same as that observed for the labeling of equilibrium-unfolded protein (6.4 s^{-1}), and only the amplitude of the labeling reaction increases with time of application of the labeling pulse.

of the unfolding molecules become labeled by DTNB in the burst phase (see Discussion).

Pulse-labeling *versus* fluorescence monitored kinetics

Figure 6(a) shows the rates of unfolding of C82A monitored by measurement of the change in reactivity of Cys40 as well as measurement of change in intrinsic tryptophan fluorescence at different urea concentrations. It is seen that the rate of unfolding monitored by probing the reactivity of Cys40 is two- to eightfold slower than the rate of unfolding monitored by tryptophan fluorescence. The observable part of the unfolding kinetics therefore indicates that the tryptophan residues get exposed to solvent much earlier than Cys40. Figure 6(b) compares the rate of unfolding of C40A monitored by accessibility of Cys82 to solvent to that measured by intrinsic tryptophan fluorescence at different urea concentrations. In this case, the rates of change in tryptophan fluorescence and change in Cys82 reactivity are similar.

Figure 6(c) compares the amplitude of the burst phase for unfolding measured by the change in reactivity of Cys40 in C82A to that measured by tryptophan fluorescence. Figure 6(d) does likewise for the change in reactivity of Cys82 in C40A. Observable data measured by either probe were fitted to single exponentials, and the exponentials extrapolated to $t = 0$. For the fluorescence data, the apparent burst phase amplitude was determined by subtracting the signal at $t = 0$ from the signal expected from linear extrapolation of the native protein signal (Figure 2). For the Cys reactivity data, the extrapolated value at $t = 0$ (Figure 5) indicates the burst phase amplitude. For both proteins, the amplitude of the apparent burst phase for unfolding monitored by tryptophan fluorescence shows very little dependence on urea concentration. In both cases, the burst phase amplitude, monitored by measurement of reactivities of the Cys residues, increases with increasing urea concentrations.

Discussion

Cysteine residues in proteins serve as useful probes to monitor structure formation and dissolution in kinetic studies of protein folding and unfolding. Using the method of pulse-labeling, the reactivity of a cysteine residue towards a thiol-specific reagent can be measured. This provides an additional technique to those utilizing pulse-labeling by hydrogen exchange (Udgaonkar & Baldwin, 1988; Roder *et al.*, 1988) or real-time NMR

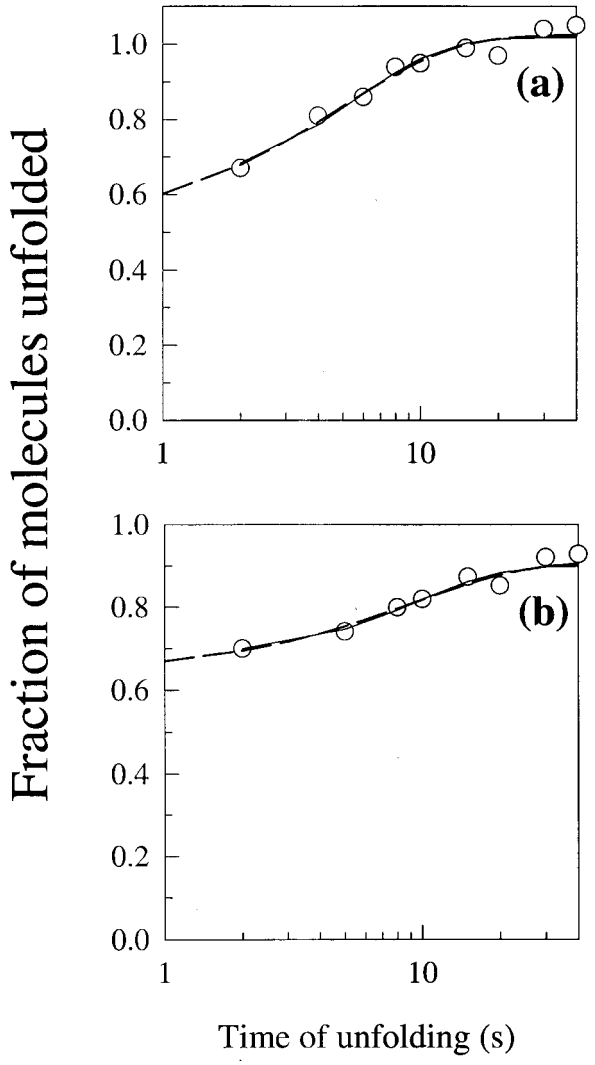

Figure 5. Kinetics of unfolding of (a) C82A and (b) C40A monitored by the pulse-labeling technique. Each protein was unfolded to a final urea concentration of 6.7 M. Each point is an average of two or three experiments. The broken lines through the data are single exponential fits to the data, and yield apparent rate constants k_5 of (a) 0.27 s^{-1} and (b) 0.19 s^{-1}. The continuous lines through the data are fits to equation (A7), using values for k_4 of 0.5 s^{-1} (C82A) and 0.23 s^{-1} (C40A) which were obtained as the rates of fluorescence changes (Figure 2) using equation (A6). The error in the determination of the extent of labeling at each time of unfolding is estimated to be ±10%, from multiple experiments.

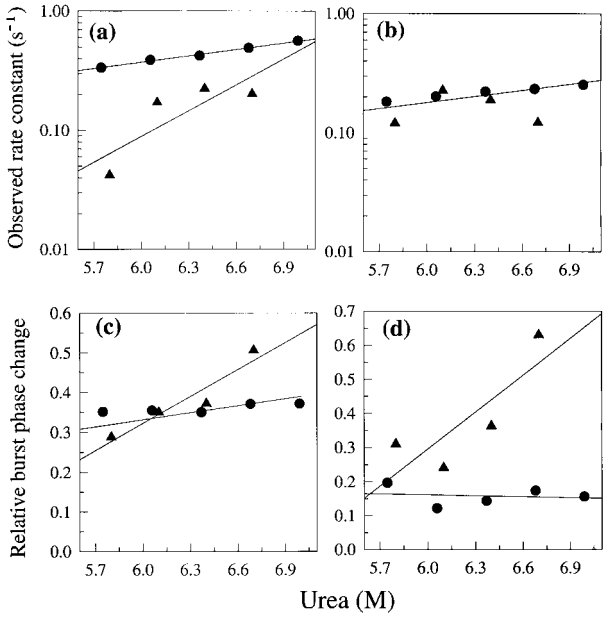

Figure 6. Kinetics of unfolding of (a) and (c) C82A, and (b) and (d) C40A, at pH 8.5 monitored by intrinsic tryptophan fluorescence *versus* pulse-labeling of a Cys thiol group. (a) and (b) Dependence of the observed rate constants on urea concentration. (c) and (d) Dependence of burst phase amplitudes on urea concentration. (●) data obtained using intrinsic tryptophan fluorescence as Data probe; (▲) data obtained using Cys thiol reactivity as a probe. The continuous lines have been drawn by inspection only. For C82A, the values of k_4 and k_5 at the different urea concentrations, obtained by fitting the changes in fluorescence and cysteine reactivity at each urea concentration to equations (A6) and (A7), are 0.34 s^{-1} and 0.05 s^{-1} (5.8 M urea), 0.4 s^{-1} and 0.18 s^{-1} (6.1 M) 0.44 s^{-1} and 0.22 s^{-1} (6.4 M), and 0.46 s^{-1} and 0.27 s^{-1} (6.7 M), respectively. For C40A, the values of k_4 and k_5 at the different urea concentrations, obtained by fitting the changes in fluorescence and cysteine reactivity at each urea concentration to equations (A6) and (A7) are 0.19 s^{-1} and 0.16 s^{-1} (5.8 M urea), 0.21 s^{-1} and 0.23 s^{-1} (6.1 M), 0.23 s^{-1} and 0.24 s^{-1} (6.4 M), and 0.234 s^{-1} and 0.2 s^{-1} (6.7 M).

(Kiefhaber *et al.*, 1995; Hoeltzli & Frieden, 1995; Bhuyan & Udgaonkar, 1999a, 2000) for probing for what occurs at a particular site in a protein during folding and unfolding. Here, the unfolding reaction has been probed using this technique because the rate of unfolding is slow enough for the well-characterized thiol reagent DTNB to be used. Observed rates of unfolding are in the range 0.1 to 0.5 s^{-1} (Figures 2 and 6) while the rate constant of reaction of DTNB with a cysteine thiol group in protein unfolded in 6.1 M urea is 6 to 30-fold faster at 3 s^{-1} (Figure 3). Thus, the number of unfolded molecules is not expected to change significantly during the pulse-labeling step, which is approximately one second.

The folding reaction of barstar is considerably faster, with the fastest observable rate being approximately 30 s^{-1} (Shastry *et al.*, 1994; Shastry & Udgaonkar, 1995), and it is clear that slow thiol-modifying reagents such as DTNB or pyridine disulfide cannot be used to probe folding reactions. Other thiol reagents such as the thiosulfonates (Roberts *et al.*, 1986; Rothwarf & Scheraga, 1991), which react with thiol groups in less than a millisecond, can be used to study fast folding reactions (Ha & Loh, 1998).

Pulse-labeling by thiol exchange with DTNB *versus* pulse-labeling by hydrogen exchange

The advantage of pulse-labeling of Cys thiol groups by DTNB over pulse-labeling by hydrogen exchange is that in the former case it is possible to monitor not only the extent of the reaction of the thiol with the label but also the rate of reaction (Figure 4). The rate of reaction of the thiol can provide information about intermediate forms with cysteine thiol-reactivities distinct from the native and the unfolded state. In the results presented here, the rate of reaction with DTNB of Cys40 in C82A or of Cys82 in C40A at any time of unfolding is the same as that seen when the protein is completely unfolded in the same concentration of denaturant used in the kinetic experiment. This result suggests that the form of protein with which DTNB reacts at any time of unfolding, has its lone cysteine thiol group in the same environment as the completely unfolded protein, U. If the environment were different from that in U, then the reactivity of the cysteine thiol group would also be expected to be different, because its reactivity depends on its pK_a, which can be significantly affected by its immediate environment (Li *et al.*, 1993).

There are two other advantages of the cysteine modification protocol over the hydrogen exchange protocol: (i) as long as the cysteine modification reaction is much faster than the folding reaction, it does not matter what happens to the protein after the labeling pulse. The protein need not even complete folding; and (ii) the use of fast cysteine-modifying agents, such as the thiosulfonates, in conjunction with a full range of single cysteine-containing mutants should make it possible to determine whether surface residues get transiently buried during folding and thus, address the question as to whether non-native structures form during folding.

A possible complication in the interpretation of experiments utilizing pulse-labeling by cysteine thiol modification is the coupling of the folding/unfolding reaction to the cysteine modification reaction. Modification of the thiol group can perturb the equilibrium between native, intermediate and unfolded species. For example, modification of Cys40 and/or Cys82 in barstar leads to an increase in stability of the protein (Ramachandran & Udgaonkar, 1996). However, two experimental results suggest that such coupling can be ruled out in the kinetic experiments reported here. Firstly, at any time during unfolding, the rate of reaction of the cysteine thiol group is that expected for the thiol group in the completely unfolded protein. Kinetic coupling would have resulted in the rates being different, because the observed rate would then be a combination of the rate corresponding to that for completely unfolded protein and the rates for folding and unfolding. Secondly, unfolding rates measured by monitoring cysteine thiol group reactivity rates are either the same (in the case of C40A) or smaller (in the case of C82A) than rates measured by monitoring tryptophan fluorescence (Figure 5). Kinetic coupling would have resulted in faster apparent rates of unfolding. The absence of kinetic coupling suggests that under the conditions of the experiments reported here (in the presence of high concentrations of urea and [DTNB]/[Protein] $\gg 1$, and the rate of labeling $\gg$ rate of unfolding), both unfolding and labeling are essentially irreversible (see below). It should be mentioned that in studies with other proteins where such coupling might be suspected, the use of multiple thiol reagents would allow the extent of coupling to be determined.

Here, the rate of change of cysteine reactivity has been compared to the rate of change in fluorescence during unfolding for each protein. Such comparisons for the two proteins are valid because the stabilities of C40A and C82A are similar, as are their unfolding kinetics (Figure 2).

Fluorescence monitored unfolding kinetics at pH 7.0 and pH 8.5

For C82A, a sub-millisecond burst phase change appears to occur in the fluorescence monitored unfolding kinetics at pH 8.5, but not at pH 7.0, although the observed rates are not very different at the two pH values (Figure 2). In the case of C40A, apparent burst phase changes in fluorescence occur at both pH values (Figure 2). The burst phase change in fluorescence at any concentration of urea was determined as the difference between the value of the extrapolated native state fluorescence at that concentration of urea and the $t = 0$ value of the kinetic curve for unfolding in the same concentration of urea. Unfolding rates are very slow (0.1 to 0.5 s^{-1}), and the 10 ms mixing dead time cannot account for the missing amplitudes.

Inspection of the data in Figure 2 reveals, however, that the $t = 0$ signals of the kinetic curves are essentially the same as the signal for native protein in the absence of denaturant. In addition, burst phase amplitudes determined using extrapolated native protein baselines do not show any dependence on denaturant concentration (Figure 6(c) and (d)). This would imply that the stability of any burst phase intermediate is independent of denaturant concentration, which is very unlikely. It is therefore difficult to determine whether the burst phase change in fluorescence is indeed real, or an artifact caused by the slope of the native protein baseline. It should be mentioned, however, that while wild-type barstar does not display a burst phase change in fluorescence under similar conditions at pH 7.0, a single Trp-containing mutant form of the protein does, whether the slope of the native baseline is taken into account or not. In the latter case, the burst phase change increases with an increase in urea concentration in a seemingly cooperative manner (Zaidi *et al.*, 1997). Clearly, more experiments are necessary to ascertain the

significance of the apparent burst phase changes in fluorescence. It should be realized, however, that if the $t = 0$ values of kinetic curves in Figure 2(a), (c) and (d) do indeed represent the native signals in unfolding conditions, then the positive slope of the native protein baseline in each case must represent accumulation of at least one equilibrium unfolding intermediate which is more fluorescent than the native protein.

Real burst phase changes in fluorescence followed by slower changes during unfolding are not the consequence of proline isomerization leading to biphasic kinetics. The folding and unfolding kinetics of barstar show a fast and slow phase only in the transition zone where coupling between the structural transitions and isomerization of Tyr47-Pro48 occurs (Schreiber & Fersht, 1993; Shastry *et al.*, 1994). The observable phase seen in the measurements reported here (Figures 2 and 5) correspond to the fast phase (Zaidi *et al.*, 1997; Schreiber & Fersht, 1993; Shastry *et al.*, 1994). In the post transition zone, the slow phase caused by proline isomerization is not seen because coupling no longer occurs (Shastry *et al.*, 1994; Kiefhaber *et al.*, 1992) and only the kinetics of the faster structural transitions are evident.

Complex unfolding kinetics are not caused by native-state heterogeneity

Before considering a possible mechanism for unfolding, it is important to rule out the most straightforward explanation for multiple phases of unfolding, which would be that they arise from heterogeneity in the native form of barstar. For example, in the case of staphylococcal nuclease, native form heterogeneity has been demonstrated by NMR methods (Wang *et al.*, 1990), and is believed to be responsible for the observed complex unfolding kinetics (Alexandrescu *et al.*, 1990). In the case of barstar, however, three different results suggest that the native state is homogeneous. Firstly, many different heteronuclear and homonuclear NMR studies of structure and dynamics have been unable to detect heterogeneity in the native state (Bhuyan & Udgaonkar, 1998; Lubienski *et al.*, 1994). Secondly, time-resolved fluorescence studies (Swaminathan *et al.*, 1996) have shown that Trp53 in the core not only displays a single lifetime, but also a very narrow lifetime distribution. The width is very similar to that of model *N*-acetyl L-tryptophan amide in solution. This clearly shows that the core around Trp53 is a single state in N. Of course, a single fluorescence lifetime will also be seen if multiple forms interconvert faster than the decay of fluorescence. Fluorescence lifetimes are, however, in the nanosecond time domain, and fast interconversion in the nanosecond time domain would not lead to the kinetics of unfolding displaying multiple rates, because all native molecules would initially convert to the form that unfolds fastest and consequently, only a single fast unfolding reaction would be seen. Lastly, if multiple native forms were present, then the kinetics of unfolding would be expected to depend on the initial conditions prior to commencement of the unfolding reaction. When the initial conditions are, however, varied from very native-like (no denaturant present) to marginally native-like (different pre-transition zone-concentrations of denaturant present), while the final unfolding conditions are constant, the unfolding kinetics of barstar are not affected (Schreiber & Fersht, 1993; Shastry *et al.*, 1994; Shastry & Udgaonkar, 1995). Thus, it is very unlikely that the native state of barstar is heterogeneous in composition, and the complex unfolding kinetics observed are most likely to arise from multi-state unfolding of a single native form.

Mechanism of unfolding

The following experimental observations must be explained by any proposed mechanism: (i) the kinetics of unfolding monitored by measurement of Cys reactivity are biphasic, with a rapid phase followed by a slower phase. In the fast phase, only a fraction of protein molecules become reactive; (ii) the rate of unfolding of C82A monitored by measurement of Cys reactivity is slower than the rate of unfolding monitored by intrinsic tryptophan fluorescence. Thus, there are at least two slow observable unfolding reactions. The dependences on urea concentration of the two rates are different; (iii) the rate of unfolding of C40A monitored by measurement of Cys82 reactivity is the same as the rate of unfolding monitored by intrinsic tryptophan fluorescence; and (iv) apparent 10 ms burst phase changes in fluorescence might also occur during unfolding.

The following mechanism is proposed to account for the data:

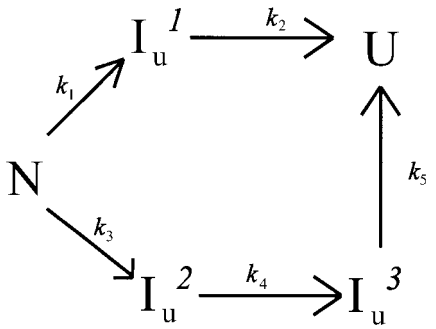

Scheme 2.

Mechanism 2 (Scheme 2) can be solved analytically to determine how the relative amounts of N, I_U^1, I_U^2, I_U^3 and U change with time during unfolding, when N is the only species present at the commencement of the unfolding reaction (Szabo, 1969). Expressions for the changes in fluorescence and cysteine reactivity with time of unfolding, that are

expected if unfolding follows mechanism 2 are given in the Appendix. The good fits of the experimental data to the expressions for the changes in fluorescence (equation (A6)) and cysteine reactivity (equation (A7)) with time of unfolding (Figure 5), demonstrate that mechanism 2 adequately and correctly describes the data.

In mechanism 2, two intermediates, I_u^1 and I_u^2, accumulate rapidly on two competing pathways of unfolding. I_U^1 exposes the thiol groups of Cys40 and Cys82 completely to solvent, while I_U^2 does not. The rates of formation of I_U^1 and I_U^2 are rapid with respect to the rates of the following conformational changes (k_1, k_3, $\gg k_2$, k_4, k_5). The extent to which they accumulate in the burst phase depends on the values of k_1 and k_3. Thus, the magnitude of the burst phase change in cysteine thiol group reactivity is given by equation (A9) (see Appendix), and its dependence on denaturant concentration is dictated by equations (A9) and (A10).

It is important to understand the necessity of including the competing pathway defined by I_U^2 and I_U^3, in mechanism 2, to account for the data presented here. In its absence, the entire change in cysteine reactivity would be expected to occur rapidly in the burst phase because all molecules would convert rapidly to I_U^1. In the presence of the competing pathway, the fraction of molecules that unfold to I_U^1 will depend on the relative values of k_1 and k_3, and is given by equation (A9).

I_U^1 and I_U^2 resemble N in their fluorescence properties: burst phase changes in fluorescence will be seen if either does not. Thus, mechanism 2 can also account for the data if the burst phase changes in fluorescence are real. It is only necessary that in equation (A1), the value of F_{I3} is not unity as is assumed in equations (A3) and (A6), but be between 1 and zero. In that case, the dependences on urea concentration of the burst phase changes in fluorescence will be different from those seen for burst phase changes in reactivities of Cys thiol groups (Figure 6), because the dependences on denaturant concentration of k_1 and k_3 are different.

It is necessary to include the intermediate I_U^3 in mechanism 2, because in its absence, the rates of fluorescence change and Cys exposure cannot be different, as is observed (Figure 6). If I_U^3 resembles U in its fluorescence properties, and N in the extent it exposes Cys40, then the rate of observable fluorescence change will be faster than the rate of Cys40 exposure in C82A, if k_2, $k_4 > k_5$. According to mechanism 2, the rate of observable fluorescence change is determined by k_4 (equation (A6)), while the rate of observable change in cysteine exposure is determined principally by k_4 and k_5 (equation (A7)). Thus, at any denaturant concentration, the rate of fluorescence change yields k_4 (Figure 6), and using the value of k_4 so obtained, the value of k_5 can be obtained by fitting the change in cysteine exposure with time to equation (A7). The values of k_4 and k_5 have different dependences on denaturant concentration as given by equation (A10); thus, the observable rates of fluorescence change and of exposure of Cys thiol groups have different dependences on denaturant concentration.

According to mechanism 2, the observed rates of cysteine exposure and fluorescence change are identical for C40A because $k_4 \approx k_5$. An alternative explanation for identical rates of cysteine exposure and fluorescence change in C40A is that in mechanism 2, I_U^2 and not I_U^1 has Cys82-exposed. In this alternative scenario, only Cys40 would get exposed in the $N \rightarrow I_U^1$ and $I_U^3 \rightarrow U$ transitions, as described in the Appendix, while Cys82 would get exposed instead in the $N \rightarrow I_U^2$ and $I_U^1 \rightarrow U$ transitions. The data do not rule out this alternative, but less simple, possibility.

Mechanism 2 is similar to mechanism 1, proposed earlier to explain CD and fluorescence studies of unfolding of wild-type as well as mutant barstar, except that the chemical labeling studies reported here suggest that the early intermediates I_U^1 and I_U^2 cannot be in rapid equilibrium with N, as suggested from the earlier studies where only spectroscopic methods were used (Zaidi *et al.*, 1997). If a rapid equilibrium between N, I_U^1 and I_U^2 were to be established before further slow conformational changes, then essentially all of the protein molecules should react rapidly with DTNB, because they would be sampling the I_U^1 conformational state at a rate that is much faster than the labeling reaction. This is a consequence of the equilibrium population being probed with an essentially irreversible chemical reaction: all molecules should react as they sample the reactive conformation. This is an important difference between using a conventional spectroscopic probe such as CD, and the chemical probe used here.

It is important to note that under the strongly denaturing conditions of our experiments, the backward (folding) reactions in mechanism 2 are expected to be slow compared to the corresponding unfolding reactions. The rates of the backward transitions, $I_U^1 \rightarrow N$ and $I_U^3 \rightarrow N$, must not only be slower than k_1 and k_3, but they must also be slower than k_2, k_4 and k_5; otherwise all protein molecules will be labeled with DTNB, as described above. Thus, backward reactions have not been considered in mechanism 2.

Structural properties of I_U^1

I_U^1 must resemble N in its fluorescence properties. Since the fluorescence of barstar has predominant contributions from Trp53 (Nath & Udgaonkar, 1997) which is completely buried in the core of the protein, this suggests that the core of the protein is still sufficiently intact in I_U^1 that Trp53 remains secluded from water. The reactivities of Cys40 and Cys82 in I_U^1 are the same as that in U, suggesting that their solvent-exposures as well as immediate environments in I_U^1 resemble those in U. The two cysteine residues are located in two separate hydrophobic pockets in the protein structure: Cys40 is located in helix 2, and Cys82 is located in the loop between helix 4 and the last

strand of the three-stranded β-sheet (Figure 1). It is possible to conjecture that these elements of secondary structure are missing in I_U^1 as they are in U, so that the reactivities of the Cys thiol groups in I_U^1 are the same as they are in U. More experiments with other single Cys-containing mutant forms of barstar are necessary to determine the validity of this hypothesis.

Fluorescence is a commonly used probe to monitor the kinetics of refolding and unfolding of proteins. It is observed that for barstar, Cys40 becomes accessible to solvent much more slowly than the tryptophan residues in the protein, monitored by their fluorescence. Thus, the use of the cysteine pulse-labeling technique indicates that fluorescence does not monitor complete unfolding, and that fluorescence sensitive conformational changes are followed by fluorescence-insensitive conformational changes. The results therefore illustrate the need to use multiple probes to monitor the kinetics of folding and unfolding, and demonstrate the occurrence of conformational changes after all spectroscopic changes have taken place.

Energy landscapes for protein folding and unfolding

From the energy landscape perspective, the accumulation of partially folded intermediate forms during folding occurs because of local stable minima, and attests to the ruggedness of the energy surface (Dill & Chan, 1997; Chan & Dill 1998; Pande *et al*., 1998; Onuchic *et al*., 1997; Dobson *et al*., 1998). A change in pH conditions, temperature, or chemical denaturant concentration, sufficient to cause the unfolding of a protein is expected to change the stabilities of such intermediates; hence, local energy minima originally present may disappear, while new local energy minima might appear. Thus, the ruggedness of the energy landscape is expected to be evident in unfolding conditions (Dill & Chan, 1997; Chan & Dill, 1998; Pande *et al*., 1998), but there are no studies applying the perspective of energy landscapes to protein unfolding reactions. The results here demonstrate that unfolding reactions can be as complex as folding reactions, suggesting that energy landscapes accessible to protein molecules during unfolding can be as intricate as those accessible during folding. It will be important to compare these energy landscapes in future studies.

Materials and Methods

C82A and C40A were purified as described (Ramachandran & Udgaonkar, 1996). Concentrations of urea (Gibco BRL) in solutions were determined by refractive index measurement on an Abbe type refractometer (Milton Roy). Experiments at pH 7.0 were carried out in solutions containing 20 mM sodium phosphate buffer and those at pH 8.5 were carried out in solutions containing 0.1 M Tris. All solutions contained 500 μM EDTA. All experiments were carried out at 25 °C.

Equilibrium and kinetic unfolding experiments

Equilibrium unfolding experiments were carried out by monitoring fluorescence of the protein at different urea concentrations. In all experiments, the protein was allowed to equilibrate for at least three hours prior to measurement. Fluorescence was monitored on a Spex DM3000 Fluorolog spectrofluorimeter. The protein sample was excited at 287 nm and emission monitored at 320 nm. The excitation and emission band widths were 0.35 nm and 10 nm, respectively. Measurements were made with a protein concentration of 2 μM and a 1 cm pathlength cuvette.

Kinetic unfolding experiments, using intrinsic tryptophan fluorescence as a probe, were carried out on a Biologic SFM-3 stopped flow machine. The excitation and emission wavelengths were 287 nm and 320 nm, respectively. The concentration of protein used was 10 μM in a 0.15 cm path-length cuvette.

Reactions of cysteine residues in C82A and C40A with DTNB

Fully folded proteins, or proteins completely unfolded in 5.8, 6.1, 6.4 or 6.7 M urea were reacted with DTNB at pH 8.5. The concentration of protein used was 15 μM and the DTNB concentration was 1.5 mM. The reaction of native protein with DTNB was done on a Genesys spectrophotometer (Milton Roy). The reaction of protein unfolded in different concentrations of urea was carried out on a Biologic SFM-3 stopped-flow machine with a mixing dead time of 10 ms.

Pulse-labeling experiments

Pulse-labeling experiments were carried out on either a Biologic SFM-3 or SFM-4 stopped-flow machine. The experiment was carried out by starting with native protein and unfolding the protein to different final concentrations of urea in an aging loop (volume of 150 μl). At different times after initiation of unfolding, the unfolding protein was pulsed with DTNB in a second mixing event. The reaction of DTNB was monitored by the change in absorbance at 412 nm as a function of time. The fraction of molecules in which the Cys residue is exposed was calculated using an extinction coefficient of 13700 M^{-1} cm^{-1} for the thionitrobenzoate ion (Riddles *et al*., 1983), released stoichiometrically on the reaction of DTNB with cysteine residues.

Analysis of kinetic data from fluorescence

All kinetic data obtained by monitoring tryptophan fluorescence were fit to single exponentials using equation (A6).

Analysis of pulse-labeling data

Raw light intensity data from pulse-labeling experiments were converted to absorbance using equation (1):

$$A_{\mathrm{PROT}} = \log\left(\frac{I_{\mathrm{DTNB}}}{I_{\mathrm{PROT}}}\right) \quad (1)$$

I_{DTNB} represents the intensity (in V) of the transmitted light for DTNB alone and I_{PROT} represents the intensity of transmitted light in the presence of DTNB and protein.

At each time of unfolding, the trace of absorbance *versus* time of labeling was fitted to a single exponential. The absorbance value at $t = \infty$, Y_∞, obtained at each unfolding time represents the extent of labeling at that time of unfolding. Plots of extent of labeling *versus* the time of unfolding were then fit to equation (A7).

Acknowledgments

We thank G. Krishnamoorthy, M.K. Mathew and R. Varadarajan for discussions. This work was funded by the Tata Institute of Fundamental Research, the Department of Biotechnology, Government of India, and the Wellcome Trust. J.B.U. is the recipient of a Swarnajayanti Fellowship from the Government of India.

References

Agashe, V. R. & Udgaonkar, J. B. (1995). Thermodynamics of denaturation of barstar: evidence for cold denaturation and evaluation of the interaction with guanidine hydrochloride. *Biochemistry,* **34**, 3286-3299.

Agashe, V. R., Shastry, M. C. & Udgaonkar, J. B. (1995). Initial hydrophobic collapse in the folding of barstar. *Nature,* **377**, 754-757.

Alexandrescu, A. T., Hinck, A. P. & Markley, J. L. (1990). Coupling between local structure and global stability of a protein: mutants of staphylococcal nuclease. *Biochemistry,* **29**, 4516-4525.

Bai, Y., Sosnick, T. R., Mayne, L. & Englander, S. W. (1995). Protein folding intermediates: native-state hydrogen exchange. *Science,* **269**, 192-197.

Ballery, N., Desmadril, M., Minard, P. & Yon, J. M. (1993). Characterization of an intermediate in the folding pathway of phosphoglycerate kinase: chemical reactivity of genetically introduced cysteinyl residues during the folding process. *Biochemistry,* **32**, 708-714.

Bhuyan, A. K. & Udgaonkar, J. B. (1998). Two structural subdomains of barstar detected by rapid mixing NMR measurement of amide hydrogen exchange. *Proteins,* **30**, 295-308.

Bhuyan, A. K. & Udgaonkar, J. B. (1999a). Observation of multistate kinetics during the slow folding and unfolding of barstar. *Biochemistry,* **38**, 9158-9168.

Bhuyan, A. K. & Udgaonkar, J. B. (1999b). Real-time NMR measurements of protein folding and hydrogen exchange dynamics. *Curr. Sci.* **77**, 942-950.

Bryngelson, J. D. & Wolynes, P. G. (1987). Spin glasses and the statistical mechanics of protein folding. *Proc. Natl Acad. Sci. USA,* **84**, 7524-7528.

Bryngelson, J. D., Onuchic, J. N., Socci, N. D. & Wolynes, P. G. (1995). Funnels, pathways, and the energy landscape of protein folding: a synthesis. *Proteins: Struct. Funct. Genet.* **21**, 167-195.

Chan, H. S. & Dill, K. A. (1998). Protein folding in the landscape perspective: chevron plots and non-Arrhenius kinetics. *Proteins: Struct. Funct. Genet.* **30**, 2-33.

Dill, K. A. & Chan, H. S. (1997). From Levinthal to pathways to funnels. *Nature Struct. Biol.* **4**, 10-19.

Dobson, C. M., Sali, A. & Karplus, M. (1998). Protein folding: a perspective from theory and experiment. *Angew. Chem. Int. Ed.* **37**, 868-893.

Goldenberg, D. P. & Creighton, T. E. (1985). Energetics of protein structure and folding. *Biopolymers,* **24**, 167-182.

Goto, Y. & Hamaguchi, K. J. (1982). Unfolding and refolding of the reduced constant fragment of the immunoglobulin light chain. Kinetic role of the intrachain disulfide bond. *J. Mol. Biol.* **156**, 911-926.

Ha, J. H. & Loh, S. N. (1998). Changes in side-chain packing during apomyoglobin folding characterized by pulsed thiol-disulfide exchange. *Nature Struct. Biol.* **5**, 730-737.

Hoeltzli, S. D. & Frieden, C. (1995). Stopped-flow NMR spectroscopy: real-time unfolding studies of 6-19F-tryptophan-labeled *Escherichia coli* dihydrofolate reductase. *Proc. Natl Acad. Sci. USA,* **92**, 9318-9322.

Kiefhaber, T., Labhardt, A. M. & Baldwin, R. L. (1995). Direct NMR evidence for an intermediate preceding the rate-limiting step in the unfolding of ribonuclease A. *Nature,* **375**, 513-515.

Kiefhaber, T., Kohler, H. H. & Schmid, F. X. (1992). Kinetic coupling between protein folding and prolyl isomerization. I. Theoretical models. *J. Mol. Biol.* **224**, 217-229.

Kraulis, P. J. (1991). MOLSCRIPT - a program to produce both detailed and schematic plots of protein structures. *J. Appl. Crystallog.* **24**, 946-950.

Li, H., Hanson, C., Fuchs, J. A., Woodward, C. & Thomas, G. J., Jr (1993). Determination of the pK_a values of active-center cysteines, cysteines 32 and 35, in *Escherichia coli* thioredoxin by Raman spectroscopy. *Biochemistry,* **32**, 5800-5808.

Lubienski, M. J., Bycroft, M., Freund, S. M. & Fersht, A. R. (1994). Three-dimensional solution structure and ^{13}C assignment of barstar using nuclear magnetic resonance spectroscopy. *Biochemistry,* **33**, 8866-8877.

Nath, U. & Udgaonkar, J. B. (1997). Folding of tryptophan mutants of barstar: evidence for an initial hydrophobic collapse on the folding pathway. *Biochemistry,* **36**, 8602-8610.

Nath, U., Agashe, V. R. & Udgaonkar, J. B. (1996). Initial loss of secondary structure in the unfolding of barstar. *Nature Struct. Biol.* **3**, 920-923.

Onuchic, J. N., Luthey-Schulten, Z. & Wolynes, P. G. (1997). Theory of protein folding: the energy landscape perspective. *Annu. Rev. Phys. Chem.* **48**, 545-600.

Pande, V. S., Grosberg, A. Y., Tanaka, T. & Rokhsar, D. S. (1998). Pathways for protein folding: is a new view needed? *Curr. Opin. Struct. Biol.* **8**, 68-79.

Phillips, C. M., Mizutani, Y. & Hochstrasser, R. M. (1995). Ultrafast thermally induced unfolding of RNase A. *Proc. Natl Acad. Sci. USA,* **92**, 7292-7296.

Ratnaparkhi, G. S., Ramachandran, S., Udgaonkar, J. B. & Varadarajan, R. (1998). Discrepancies between the NMR and X-ray structures of uncomplexed barstar: analysis suggests that packing densities of protein structures determined by NMR are unreliable. *Biochemistry,* **37**, 6958-6966.

Ramachandran, S. & Udgaonkar, J. B. (1996). Stabilization of barstar by chemical modification of the buried cysteines. *Biochemistry,* **35**, 8776-8785.

Riddles, P. W., Blakeley, R. L. & Zerner, B. (1983). Reassessment of Ellman's reagent. *Methods Enzymol.* **91**, 49-60.

Roberts, D. D., Lewis, S. D., Ballou, D. P., Olson, S. T. & Shafer, J. A. (1986). Reactivity of small thiolate anions and cysteine-25 in papain toward methyl methanethiosulfonate. *Biochemistry*, **25**, 5595-5601.
Roder, H., Elove, G. A. & Englander, S. W. (1988). Structural characterization of folding intermediates in cytochrome c by H-exchange labeling and proton NMR. *Nature*, **335**, 700-704.
Rothwarf, D. M. & Scheraga, H. A. (1991). Regeneration and reduction of native bovine pancreatic ribonuclease A with oxidized and reduced dithiothreitol. *J. Am. Chem. Soc.* **113**, 6293-6294.
Sali, A., Shakhnovich, E. & Karplus, M. (1994). How does a protein fold? *Nature*, **369**, 248-251.
Schreiber, G. & Fersht, A. R. (1993). The refolding of *cis*- and *trans*-peptidyl prolyl isomers of barstar. *Biochemistry*, **32**, 11195-11203.
Segawa, S. & Sugihara, M. (1984a). Characterization of the transition state of lysozyme unfolding. I. Effect of protein-solvent interactions on the transition state. *Biopolymers*, **23**, 2473-2488.
Segawa, S. & Sugihara, M. (1984b). Characterization of the transition state of lysozyme unfolding. II. Effects of the intrachain crosslinking and the inhibitor binding on the transition state. *Biopolymers*, **23**, 2489-2498.
Shastry, M. C. & Udgaonkar, J. B. (1995). The folding mechanism of barstar: evidence for multiple pathways and multiple intermediates. *J. Mol. Biol.* **247**, 1013-1027.
Shastry, M. C., Agashe, V. R. & Udgaonkar, J. B. (1994). Quantitative analysis of the kinetics of denaturation and renaturation of barstar in the folding transition zone. *Protein Sci.* **3**, 1409-1417.
Swaminathan, R., Nath, U., Udgaonkar, J. B., Periasamy, N. & Krishnamoorthy, J. (1996). Motional dynamics of a buried tryptophan reveal the presence of partially structured forms during denaturation of barstar. *Biochemistry*, **35**, 9150-9157.
Szabo, Z. G. (1969). Kinetic characterization of complex reaction systems. In *Comprehensive Chemical Kinetics* (Bamford, C. H. & Tipper, C. F. H., eds), vol. 2, pp. 1-80, Elsevier, New York, USA.
Udgaonkar, J. B. & Baldwin, R. L. (1988). NMR evidence for an early framework intermediate on the folding pathway of ribonuclease A. *Nature*, **335**, 694-699.
Wang, J. F., Finck, A. P., Loh, S. N. & Markley, L. (1990). Two dimensional NMR studies on staphylococcal nuclease: evidence for conformational heterogeneity from hydrogen-1 carbon-13 and nitrogen-15 spin system assignments of the aromatic amino acids in the nuclease H124L-thymidine 3′,5′ bisphosphate-Ca + 2 ternary complex. *Biochemistry*, **29**, 4242-4253.
Xu, Y., Mayne, L. & Englander, S. W. (1998). Evidence for an unfolding and refolding pathway in cytochrome *c*. *Nature Struct. Biol.* **5**, 774-778.
Zaidi, F. N., Nath, U. & Udgaonkar, J. B. (1997). Multiple intermediates and transition states during protein unfolding. *Nature Struct. Biol.* **4**, 1016-1024.

Appendix

According to mechanism 2 (see the main text), the changes in fluorescence, $F(t)$, and cysteine exposure, $C(t)$ during unfolding are given by:

$$F(t) = F_N \times N(t) + F_{I1} \times I_U^1(t) + F_{I2} \times I_U^2(t) + F_{I3} \times I_U^3(t) + F_U \times U(t) \quad \text{(A1)}$$

$$C(t) = C_N \times N(t) + C_{I1} \times I_U^1(t) + C_{I2} \times I_U^2(t) + C_{I3} \times I_U^3(t) + F_U \times U(t) \quad \text{(A2)}$$

where F_i refers to the fluorescence signal corresponding to 1 mol of species i, C_i refers to the cysteine exposure of 1 mol of species i, and $i(t)$ represents the concentration of species i at time t of unfolding.

Mechanism 2 will account for the observed changes in fluorescence with the simple assumption that they take place only during the $I_U^1 \rightarrow U$ and $I_U^2 \rightarrow I_U^3$ transitions, so that $F_N = F_{I1} = F_{I2} = 1$ and $F_{I3} = F_U = 0$. It will account for the observed changes in cysteine exposure with the assumption that these take place in the $N \rightarrow I_U^1$ and $I_U^3 \rightarrow U$ transitions so that $C_N = C_{I2} = C_{I3} = 0$ and $C_{I1} = C_U = 1$. Then, the observed changes in fluorescence and cysteine exposure are given by:

$$F(t) = N(t) + I_U^1(t) + I_U^2(t) \quad \text{(A3)}$$

$$C(t) = I_U^1(t) + U(t) \quad \text{(A4)}$$

The combination of parallel and consecutive reactions in mechanism 2 have exact analytical solutions for $N(t)$, $I_U^1(t)$, $I_U^2(t)$, $I_U^3(t)$ and $U(t)$, as described by Szabo (1969) and Shastry & Udgaonkar (1995). The expressions become simpler when $k_1, k_3 \gg k_2, k_4, k_5$, and for $t \gg k_1^{-1}$, k_2^{-1}. Under these conditions, the expression for $F(t)$ simplifies to:

$$F(t) = \left(\frac{k_1}{k_1 + k_3} e^{-k_2 t} + \frac{k_3}{k_1 + k_3} e^{-k_4 t}\right) A_0 \quad \text{(A5)}$$

Furthermore, if $k_2 = k_4$:

$$F(t) = A_0 e^{-k_4 t} \quad \text{(A6)}$$

The expression for $C(t)$ is given by:

$$C(t) = \left(1 - \frac{k_3}{k_1 + k_3} \frac{k_5 e^{-k_4 t} - k_4 e^{-k_5 t}}{k_5 - k_4}\right) A_0 \quad \text{(A7)}$$

Furthermore, if $k_4 \gg k_5$:

$$C(t) = A_0 \left(1 - \frac{k_3}{k_1 + k_3} e^{-k_5 t}\right) \quad \text{(A8)}$$

From equation (A7), the burst phase change in cysteine activity is given by:

$$C(t) = A_0 \left(1 - \frac{k_3}{k_1 + k_3}\right) = A_0 \left(\frac{k_1}{k_1 + k_3}\right) \quad \text{(A9)}$$

The increase in the microscopic rate constants of unfolding, k_i, of mechanism 2, with increase in denaturant concentration, is given by Tanford (1970):

$$\log k_i = \log k_i^0 + m_{k_i}[D] \quad \text{(A10)}$$

where k_i^0 is the rate constant of unfolding in the absence of denaturant, and m_{ki} is the slope of the linear dependence of log λ_2 on the concentration of denaturant.

References

Shastry, M. C., & Udgaonkar, J. B. (1995). The folding mechanism of barstar: evidence for multiple pathways and multiple intermediates. *J. Mol. Biol.* **247**, 1013-1027.

Szabo, Z. G. (1969). Kinetic characterization of complex reaction systems. In *Comprehensive Chemical Kinetics* (Bamford, C. H. & Tipper, C. F. H., eds), vol. 2, pp. 1-80, Elsevier, New York, USA.

Tanford, C. (1970). Protein denaturation. Part C. Theoretical models for the mechanism of denaturation. *Advan. Protein Chem.* **21**, 1-95.

Edited by C. R. Matthews

(Received 14 October 1999; received in revised form 3 February 2000; accepted 8 February 2000)